Correlation of Optical Coherence Tomography and Autofluorescence in the Outer Retina and Choroid of Patients With Choroideremia

Kanmin Xue, Marta Oldani, Jasleen K. Jolly, Thomas L. Edwards, Markus Groppe, Susan M. Downes, and Robert E. MacLaren

Nuffield Laboratory of Ophthalmology, University of Oxford & Oxford Eye Hospital, John Radcliffe Hospital, Oxford University Hospitals NHS Trust, Oxford, United Kingdom

Correspondence: Kanmin Xue, Academic Clinical Lecturer, Nuffield Laboratory of Ophthalmology, Level 6 West Wing, John Radcliffe Hospital, Headley Way, Oxford OX3 9DU, UK;
kanmin.xue@ouh.nhs.uk.

KX and MO are joint first authors.

Submitted: October 8, 2015
Accepted: May 22, 2016

Citation: Xue K, Oldani M, Jolly JK, et al. Correlation of optical coherence tomography and autofluorescence in the outer retina and choroid of patients with choroideremia. *Invest Ophthalmol Vis Sci*. 2016;57:3674–3684. DOI:10.1167/iovs.15-18364

Purpose. To evaluate the relationships between RPE, photoreceptor, and choroidal degeneration in choroideremia.

Methods. Enhanced-depth imaging optical coherence tomography (EDI-OCT), scanning laser ophthalmoscopy (SLO), and autofluorescence (AF) were performed on 39 patients (78 eyes) with choroideremia. The edges of surviving outer retina on OCT and residual AF were aligned. The distribution of outer retinal tubulations was mapped over a range of ages (16–71 years), and comparison made between pre- and postsubretinal gene therapy. Subfoveal choroidal thickness (SFCT) was compared between 23 choroideremia patients (42 eyes) and 20 age- and refraction-matched male controls (40 eyes).

Results. The edges of RPE AF aligned with a reduction in outer nuclear layer thickness (Spearman's rho = 0.9992). Correlation was also found between the quality of AF and integrity of ellipsoid zone within islands of surviving retina. Tubulations existed in 71 of 78 (91%) eyes with choroideremia and remained stable following gene therapy. Subfoveal choroidal thickness was reduced at baseline in choroideremia (179.7 ± 17.2 μm) compared with controls (302.0 ± 4.8 μm; $P < 0.0001$), but did not undergo significant thinning until end-stage retinal degeneration (43.1 ± 6.5 μm).

Conclusions. The data suggest that RPE loss is the primary cause of photoreceptor degeneration in choroideremia. The choroid is thinner than controls from early stages, in keeping with a mild developmental defect. Photoreceptors appear to lose outer segments following loss of underlying RPE and form tubulations at the edges of degeneration. The preservation of tubulations over time and after subretinal injection would be consistent with these structures maintaining attachment to the inner retina and hence being potentially light responsive (ClinicalTrials.gov, NCT01461213).

Keywords: choroideremia, optical coherence tomography, autofluorescence

Choroideremia (CHM) is an X-linked retinal degeneration. Affected individuals suffer from nyctalopia during early childhood and progressive loss of peripheral visual field with age. The degeneration is characterized by gradual loss of the RPE, outer retina, and choroid, which gives rise to a characteristic atrophic fundal appearance. It is unclear whether the loss of each layer occurs sequentially due to interdependent cell survival, or independently due to shared defects in the ubiquitously-expressed Rab-escort protein (REP1) encoded by the *CHM* gene. This question is now clinically relevant, because it is important to determine which layer should be the primary target for any potential gene replacement therapy for choroideremia.

Fundus autofluorescence (AF) imaging has shown that RPE degeneration in choroideremia occurs in a centripetal fashion, with early loss of peripheral AF leading to the formation of a residual 'island' of preserved AF with sharply demarcated scalloped edges, usually centred around the fovea. The island shrinks over time and eventually encroaches on the fovea, which is associated with a sharp decline in visual acuity, generally during the fourth to fifth decade of life (Jolly et al.[1]). Changes in the size of the AF island over time could be used to monitor disease progression. However, it is unclear how alterations in AF, taken as a marker for RPE health, correlate with the state of the adjacent photoreceptors and choroid/choriocapillaris. The primary objective of this study was therefore to assess the relationship between retinal structural changes visible with optical coherence tomography (OCT) and changes in AF in choroideremia. Specifically, we investigated the relationship between outer retina integrity and RPE health at the edges of surviving AF islands in a cohort of 38 CHM patients. We also explored the association between the outer retina and choroidal thickness in CHM. Finally, we evaluated the immediate physical effects of subretinal injection on the delicate outer retina architecture at the transition zone of AF in a cohort of trial participants who underwent gene therapy.[2] Understanding these mechanisms may help in the future evaluation of retinal function following gene therapy, particularly at the periphery of the surviving island of AF.

Methods

This was a retrospective noninterventional image analysis of EDI-OCT and AF images from 39 patients with a clinical and genetic diagnosis of choroideremia at the Oxford Eye Hospital, Oxford, UK. The research was performed as part of an ongoing clinical trial (NCT01461213) approved by the national ethics committee and adhered to the Declaration of Helsinki (2013).

High-resolution spectral-domain OCT was obtained using the Spectralis HRA+OCT system (Heidelberg Engineering GmbH, Heidelberg, Germany) with 37 horizontal volume scans covering 30° × 15° centered over the foveola. Enhanced-depth imaging mode was activated during OCT capture and a simultaneous 30° × 30° infrared confocal SLO image was captured automatically. In the same sitting, a 30° × 30° BluePeak laser fundus AF image was captured using the same optics according to the manufacturer's standard operating procedure, including focusing in the red-free reflectance mode and Automated Real-Time ('ART') alignment of at least eight single images to create a mean image.

Precise point-to-point alignment of corresponding locations between OCT and AF images was performed in the Heidelberg Eye Explorer software (HEYEX; Heidelberg Engineering GmbH) in two ways using the SLO image as an intermediary. HEYEX has a sophisticated in-built image recognition and alignment capability, which allows tracking of eye movements during image acquisition. This function is also available during image analysis when a marker annotating the 30° × 30° SLO image attached to the OCT may be copied and pasted onto the corresponding 30° × 30° AF image using common landmarks as reference points in HEYEX. We confirmed the precision of this method of image alignment using an alternative manual technique. This consisted of choosing two fixed reference points (e.g., small vessel branch points) common to both the SLO and AF images. The distance between the two reference points can be measured precisely on each image using the HEYEX marker tool. The ratio of the two measurements was calculated to generate a mathematical conversion factor. A point of interest on an OCT image is automatically displayed on the linked SLO image as a crosshair in HEYEX. A pair of circles centered at the two reference points could then be drawn on the SLO image under high magnification such that they intersect exactly at the crosshair. The diameters of the circles were automatically displayed by HEYEX and used to calculate the predicted diameters of corresponding circles on the AF image by multiplying through the conversion factor. The intersection of the two circles of predicted diameters drawn on the AF image would then correspond exactly with the point of interest on the OCT.

Six choroideremia patients (aged 35–65 years) underwent gene therapy: 0.6 to 1.0 × 10^{10} genome particles of a recombinant adeno-associated viral vector encoding REP1 (AAV2-REP1) was delivered by pars plana vitrectomy and subretinal injection, as reported previously.[2] Serial images pre-, 1 month post-, and 6 months postgene therapy were obtained at the same locations using the AutoRescan function of the Spectralis by selecting the baseline image as the reference scan. All outer retinal tubulations (cystic structures) on each B-scan of the OCT were identified and mapped to corresponding positions on the AF image using the point-to-point image alignment technique described above.

Subfoveal choroidal thickness (SFCT) was defined as the distance from the outer border of the RPE to the inner scleral border directly below the foveal dip on EDI-OCT. Subfoveal choroidal thickness was measured in 23 choroideremia patients and 20 aged-matched male patients without significant retinal or choroidal pathology. All subjects had refractions between −5.5 and +5.0 diopters (D). For data analysis, choroideremia patients were further divided into three groups based on foveal outer retinal integrity being preserved, disrupted, or lost on OCT. A Kruskal-Wallis test was performed to assess the significance of any differences between the groups.

Results

Correlation Between AF and OCT Morphology

Manual and automated point-to-point alignment between outer retinal morphology on the OCT and the edges of AF islands showed consistent correspondence between the edge of AF and the beginning of an acute decline in outer nuclear layer (ONL) thickness on the OCT, which diminished to zero in a triangular slope over approximately 200 μm (Fig. 1). To test the consistency of this observation, image alignment analysis was performed using OCT and AF images from 78 eyes of 39 patients with choroideremia. Of these, the images of 49 eyes were suitable for alignment. Twenty-nine eyes were excluded from the analysis for the following reasons: (1) no outer retina remaining on OCT (due to end stage degeneration, $n = 15$), (2) poor image quality (due to poor fixation, $n = 8$), and (3) intact outer retina extending beyond the edge of captured image (usually in early disease, $n = 6$) (Table). When the transfoveal AF island widths (y) measured on AF images were compared with those predicted (y') based on the width of intact ONL on OCT (x) in all 49 eyes (see schematic illustration in Fig. 1D), the median difference was zero (range, −65 to +62 μm). In 29 (59%) eyes, an exact correspondence was found between the predicted and measured transfoveal AF island width. The overall Spearman rank correlation coefficient (rho) between measured and predicted transfoveal AF width was 0.9992. The external limiting membrane (ELM) and the ellipsoid zone (EZ) generally terminated at the same location as where the ONL thickness began to show a sharp decline.[3] The EZ and ELM were often ill defined at the edge of degeneration due to a disrupted appearance on the OCT, and were less reliable predictors of the location of the AF border.

In six eyes of three patients aged 16, 22, and 23 years, the residual AF islands consisted of an ovoid central zone of relatively preserved AF and a peripheral zone of mottled AF (Fig. 2). When these AF images were aligned to their respective OCTs, the regions with preserved AF were found to correspond to areas of the retina with preserved EZ integrity, while the surrounding region of mottled AF corresponded to areas with disrupted EZ. The horizontal diameters of the central ovoid zones with preserved AF were individual-specific but non–age-dependent: 3050 μm OD/3180 μm OS (age 16), 3250 μm OD/3050 μm OS (age 22), and 2400 μm OD/2400 μm OS (age 23). The mean eccentricities of the zones of preserved AF in relation to the anatomic foveal dip were 1533 μm (SEM = 179) nasally, 1339 (SEM = 157) temporally, and 1436 (SEM = 70) overall, which are consistent with these zones representing areas of relatively high cone density.[4,5] While such AF zonal transition was seen in three of the youngest choroideremia patients in the cohort (presumably a phenotype associated with an early stage of disease), the rest of the eyes presented with more homogeneous mottled AF over the entire island, associated with generalized EZ disruption.

Tubulations and the Effects of Gene Therapy

Outer retinal tubulations (ORT) have previously been observed in advanced AMD and other degenerative retinal conditions.[6] The mechanism of tubule formation is unclear, although it has

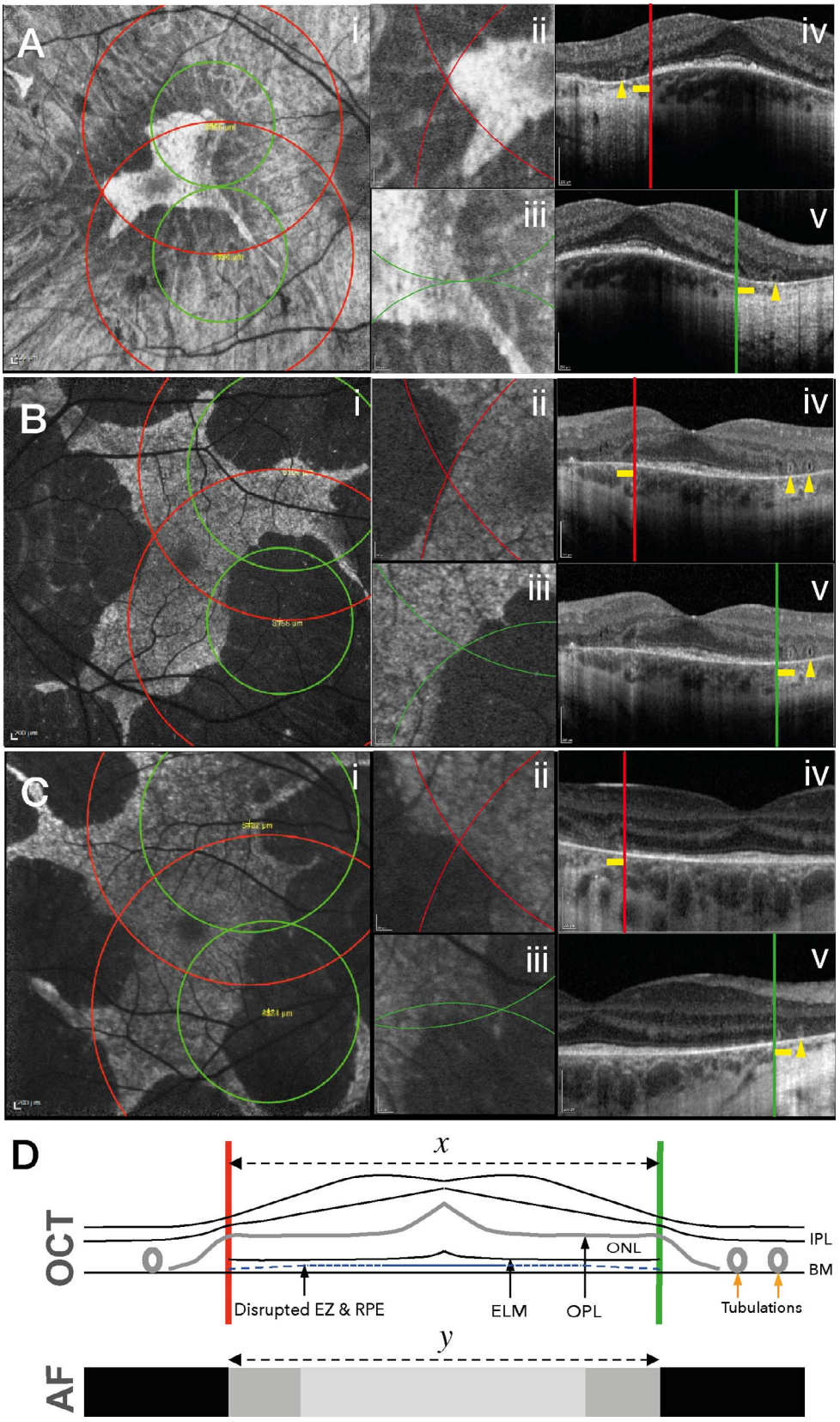

Figure 1. Correlation between edges of AF islands and OCT structural changes in choroideremia. Panels (**A**–**C**) show representative images from three choroideremia patients. By plotting pairs of intersecting *circles* of proportional diameters from fixed reference points (e.g., vessel branch points) on the AF and SLO images, precisely corresponding point locations could be identified between the AF and OCT B-scans, and vice versa. The intersection between two *red circles* on the AF image marking the left-hand border of RPE degeneration (**A***i*), with high magnification view shown (**A***ii*), corresponds to the position on the OCT indicated by a *vertical red line* (**A***iv*), while the intersection between green circles marking the right-hand border of RPE degeneration (**A***i*, **A***iii*) corresponds to a second position on the OCT indicated by a *vertical green line* (**A***v*). The same applies

Investigative Ophthalmology & Visual Science

to panels (**B**, **C**). The edges of surviving RPE on the OCT coincide with the start of an acute decline in ONL height, which diminishes to zero in a triangular transition zone, denoted by *horizontal yellow bars*. Immediately beyond the loss of ONL, outer retinal tubulations were frequently observed (*yellow arrows*). *Scale bars*: 200 μm. A summary of the characteristic OCT to AF image alignment features is provided in (**D**). Correlation between the transfoveal island width (y) measured on AF images and those predicted based on OCT outer retinal width (x) was performed in 49 choroideremia eyes (data summarized in the Table). OPL, outer plexiform layer; BM, Bruch's membrane.

been speculated to represent an arrangement of degenerating photoreceptors with potential contribution from adjacent RPE or glial elements. In our cohort of choroideremia patients, tubulations were found to be present to a variable extent on the OCT of the majority of eyes across the age range and disease severity (Fig. 3): 71 of 78 (91%) eyes examined demonstrated tubulations; one eye was not assessable due to poor image quality (Table). The six eyes that did not show any tubulations were all at end-stage degeneration with no outer retinal structure remaining. When mapped onto AF images, the tubulations seen on OCT B-scans were universally located beyond the edges of the AF islands (therefore, overlying bare Bruch's membrane), with a mean distance of approximately 400 to 500 μm from the nearest island edge, although some were significantly farther away (Fig. 3D). Even though tubulations appear to be isolated and cystic in appearance on OCT B-scans, two-dimensional analysis of their locations showed that many were in fact contiguous with the main island of surviving outer retina via 'pseudodendritic' tubular extensions (Fig. 4). These thin pseudodendrites appear to lie over areas devoid of RPE (by the absence of AF) but are detectable by their retinal pigmentation on high magnification infrared SLO images.

Because tubulations likely represent rearrangement of surviving photoreceptors, we asked whether their distribution would be affected by subretinal injections in gene therapy, because this would provide us with indirect evidence as to whether or not they might have retained synapses to the overlying retina. When the locations of tubulations were compared between baseline, 1 month, and 6 months post AAV.REP1 gene therapy, it could be seen that the general distributions of tubulations were not significantly affected by surgically induced retinal detachments (Fig. 5). Moreover, while a slight dip in the number of outer retinal cysts seen in some eyes at 1 month could be attributed to mechanical disturbance from the retinal detachment, there was no statistically significant fluctuation over the 6-month period (linear regression: $F(5,6) = 1.29$, $P = 0.38$; Supplementary Fig. S1). These would be in keeping with tubulations maintaining some physical attachment to the inner retina, thereby potentially retaining some visual function over these anatomical anomalies.

Correlation Between Choroidal Thickness and Ellipsoid Zone

Although the *CHM* gene defect is known to cause degeneration, most patients start life with good vision. We were therefore interested to know if there might be any developmental anomalies in choroideremia patients and/or if the subfoveal choroid thinning begins before significant foveal retinal degeneration is evident. Subfoveal choroidal thickness was measured in 42 eyes of 23 choroideremia patients (mean age 37.5 years; range, 12–63) and 40 eyes of 20 age-matched healthy male controls (mean age 37.6 years; range, 13–62; Supplementary Table S1). The mean refraction of CHM eyes was −0.92 D (±SEM 0.37) and control eyes −0.28 D (±SEM 0.34). Unpaired 2-tailed *t*-test showed no statistically significant difference between the refractions of the two groups ($P = 0.21$). The mean SFCT in healthy controls (302.0 μm ± 4.8 SEM) was found to be significantly greater than that in CHM eyes with preserved EZ (179.7 μm ± 17.2 SEM; $P < 0.0001$; Fig. 6). Also, the SFCT of CHM eyes with disrupted EZ (191.9 μm ± 10.8 SEM) was significantly greater than those with lost EZ (43.1 μm ± 6.5 SEM; $P < 0.0001$). However, no significant difference in SFCT was found between CHM eyes associated with preserved and disrupted EZ ($P = 0.8251$).

Discussion

The *CHM* gene product, REP1 (Rab escort protein 1), regulates the prenylation of Rab GTPases, which play important roles in intracellular vesicular trafficking. Deficiency of REP1 is thought to impair the transport of proteins from the Golgi apparatus to the outer segments in photoreceptors, as well as the phagocytosis and degradation of shed outer segments by RPE cells. Cell type-specific knockouts of *Chm* in mice have shown the potential for independent degeneration of photoreceptor and RPE layers, but the rate of degeneration was accelerated when both layers were defective simultaneously, presumably due to interdependent cell survival.[7,8] Our data revealed a precise anatomical correspondence between RPE and photoreceptor degeneration: the edge of RPE loss colocalized with a sharp decline in ONL thickness in the majority of eyes with CHM. Small sporadic discrepancies were occasionally observed, which were equivalent to the size of fewer than four RPE cells each with a diameter of approximately 15 μm.[9] These could be attributed, in part, to temperature and calibration-dependent alignment errors between simultaneous infrared and tomographic scans from the Heidelberg Spectralis system itself.[10] In the narrow transition zone between intact and degenerate outer retina, the ONL was consistently seen to taper in a triangular fashion, a feature that has previously been termed an 'interlaminar bridge'.[11,12] We hypothesize that this transition zone represents degenerating photoreceptors that reduce in height as they lose outer segments following the death of the interdigitating RPE cells, eventually leading to cell death. This would be in keeping with histopathologic observations from postmortem female carriers of choroideremia.[13]

The correlation between RPE and photoreceptor integrity was not only observed at the advancing border of degeneration, but also within the islands of surviving outer retina/RPE. Ovoid zones of parafoveal preservation of AF were seen in some of the youngest choroideremia patients in the cohort, which correlated with transitions in the integrity of the EZ. Moreover, the size and eccentricities of the ovoid zones were consistent with representing areas of relatively high cone density previously observed using histology and adaptive optics.[4,5] Taken together, the data provides indirect evidence for relative sparing of cones (and their underlying RPE) in the early stages of choroideremia. The early cone sparing may be explained by the low REP1 expression in cones versus high expression in rods.[5,12] As the disease progresses, the central preservation is lost, suggesting that cone degeneration in choroideremia may be secondary to rod or RPE degeneration. It would also explain the clinical finding of early-onset nyctalopia, but preservation of visual acuity and color perception until late stage degeneration in choroideremia patients.

Investigative Ophthalmology & Visual Science

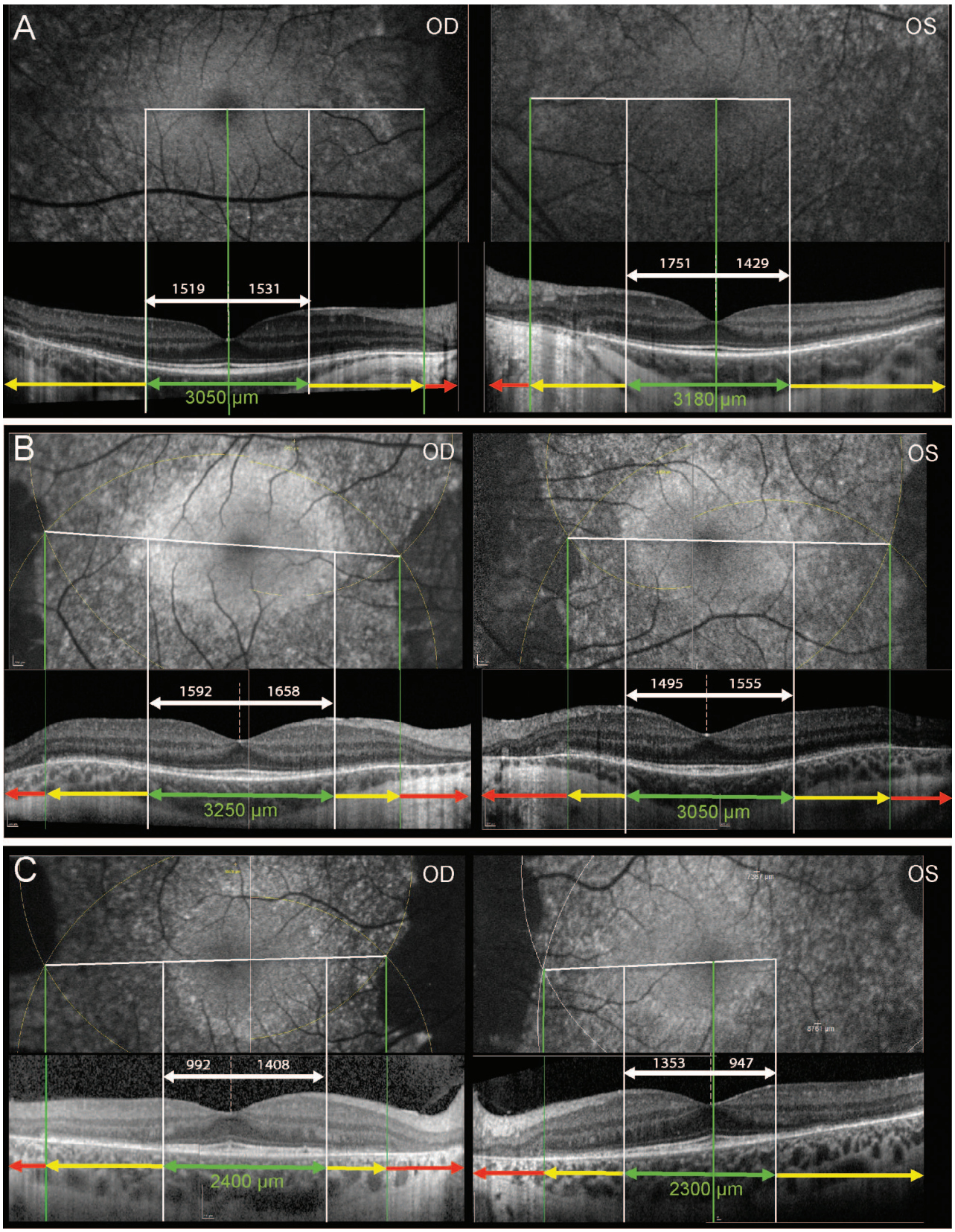

Figure 2. Correlation between the pattern of AF and integrity of the EZ. In three young choroideremia patients aged 16 (**A**), 22 (**B**), and 23 years (**C**) who have large residual islands remaining on AF imaging, central ovoid zones with relatively preserved AF were observed, which aligned with regions of preserved EZ integrity on the OCT (*green arrow bars*). The size and eccentricities of these ovoid zones in relation to the anatomical foveal dip (*white arrows*) are consistent with representing areas of greatest cone density.[4,5] The rest of the islands showed mottled AF, which corresponded to disrupted EZ (*yellow arrow bars*). Areas of absent AF corresponded to complete EZ loss (*red arrow bars*). Note that in (**A**) (OD & OS) and (**C**) (OS), at least one edge of the AF island fell outside the OCT image boundaries, therefore the foveola has been used as one of the reference points during image alignment.

Investigative Ophthalmology & Visual Science

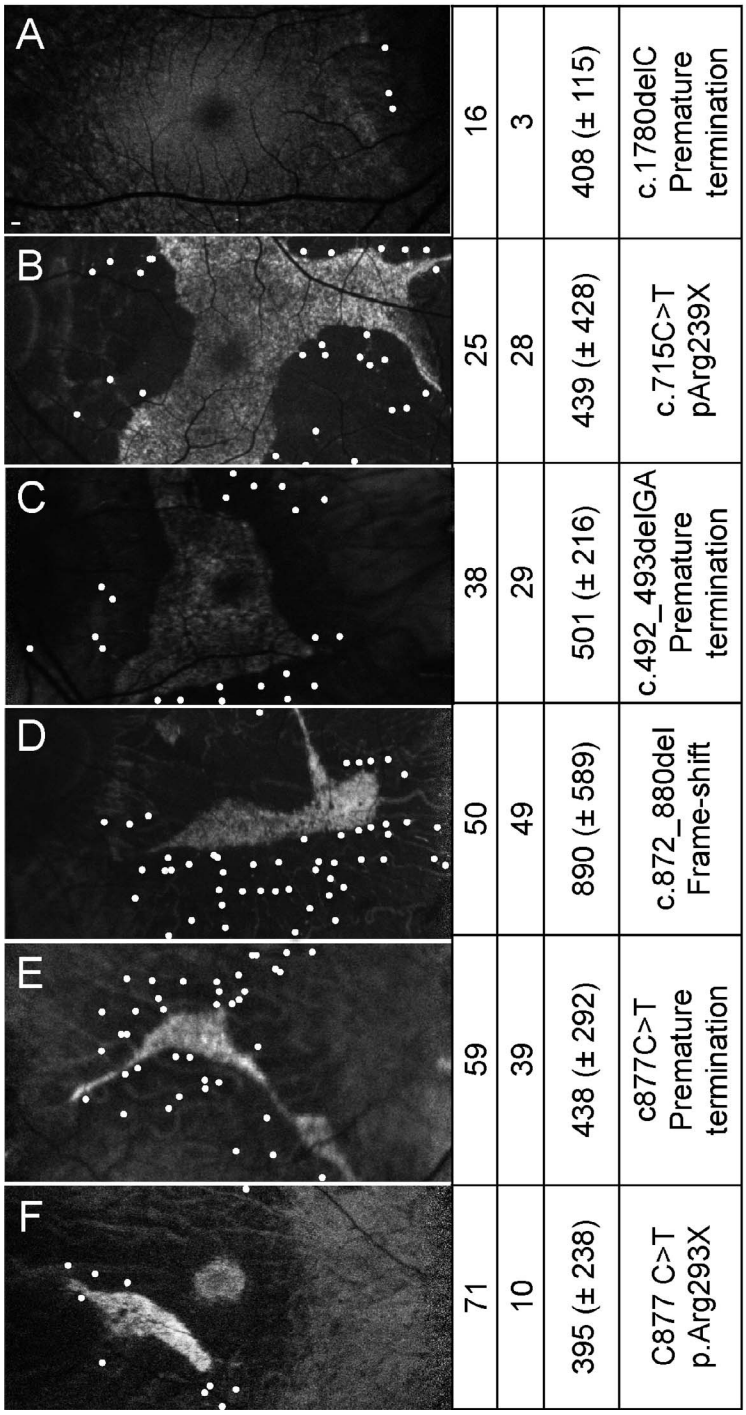

Figure 3. Distribution of outer retinal cysts in six patients with choroideremia aged 16 to 71 years ([**A**–**F**] in ascending age order). The distribution of tubulations could be inferred from the positions of all outer retinal cysts (ORCs), which represent cross-sections of tubulations, seen on all B-scans of the OCT. For each eye, all ORCs were mapped to corresponding locations on the AF image (shown as *white dots*). The Table displays the mean distance of ORCs from the nearest edge of AF island (±SD) and genetic mutations in the *CHM* gene for each patient.

Investigative Ophthalmology & Visual Science

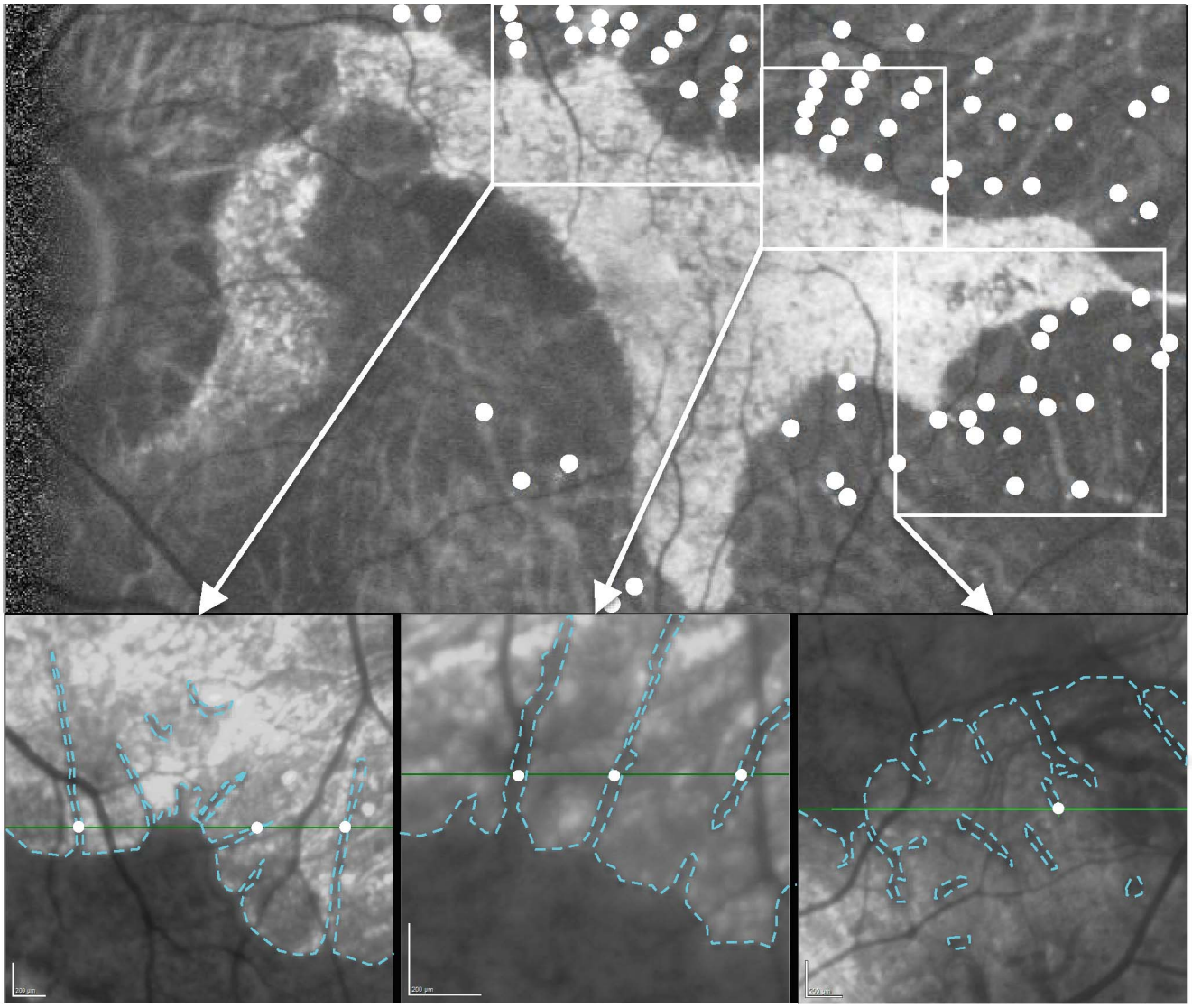

FIGURE 4. Outer retinal cysts on OCT represent cross-sections through outer retinal tubulations following RPE loss at the edges of degeneration. Plotting the locations of ORCs (*white dots*) seen on every B-scan of the OCT (*horizontal green lines*) over the corresponding high magnification infrared SLO image revealed that the ORCs lie over thin 'pseudodendrites' containing retinal pigment along the edges of the surviving retina (outlined in *dotted blue*). These pseudodendrites do not match the background autofluorescence of the choroidal vasculature (*top panel*) but represent distinct tubular outer retinal structures.

We found no significant difference between the subfoveal choroidal thickness underlying retina with preserved or disrupted EZ. The choroidal thickness only dropped once the EZ has completely degenerated. This suggests that choroidal degeneration may be a secondary phenomenon, which lags significantly behind photoreceptor (and RPE) degeneration. This would be in keeping with observations from postmortem female carriers in which choroidal thinning was only seen in areas of severe retinal degeneration.[13] We noted, however, that SFCT was reduced in early choroideremia eyes compared with controls, at a time when the EZ remained relatively intact. Although choroidal thickness is affected by age, sex, and refractive error, these factors were all similar between the CHM and control eyes in the study.[14] A possible explanation would be that the impairment of RPE due to REP1 deficiency also impairs the ability of the RPE to influence development of the choroidal vasculature long before the onset of degeneration. Alternatively, REP1 deficiency may be associated with a primary choroidal abnormality, although this is unlikely based on two observations: (1) CHM carrier females with patchy retinal degeneration due to X-inactivation do not show corresponding patchy choroidal abnormality, and (2) CHM patients occasionally present with secondary choroidal neovascularization, which suggests relatively intact choroidal angiogenesis. Nevertheless the reduced choroidal thickness at baseline did not appear to have any obvious effect on visual acuity in the early stages of the disease. Choroidal thinning has also been described as a secondary phenomenon in dry AMD, presumably as a result of degeneration of the RPE.[15] Hence, choroidal thinning in CHM appears to occur through a dual mechanism of reduced baseline thickness, which is probably not clinically significant, but which then progresses once there is loss of the overlying RPE as part of the late disease process.

Not all photoreceptors are lost beyond the edge of RPE degeneration, as some appear to survive by forming outer retinal tubulations, which could extend a considerable distance

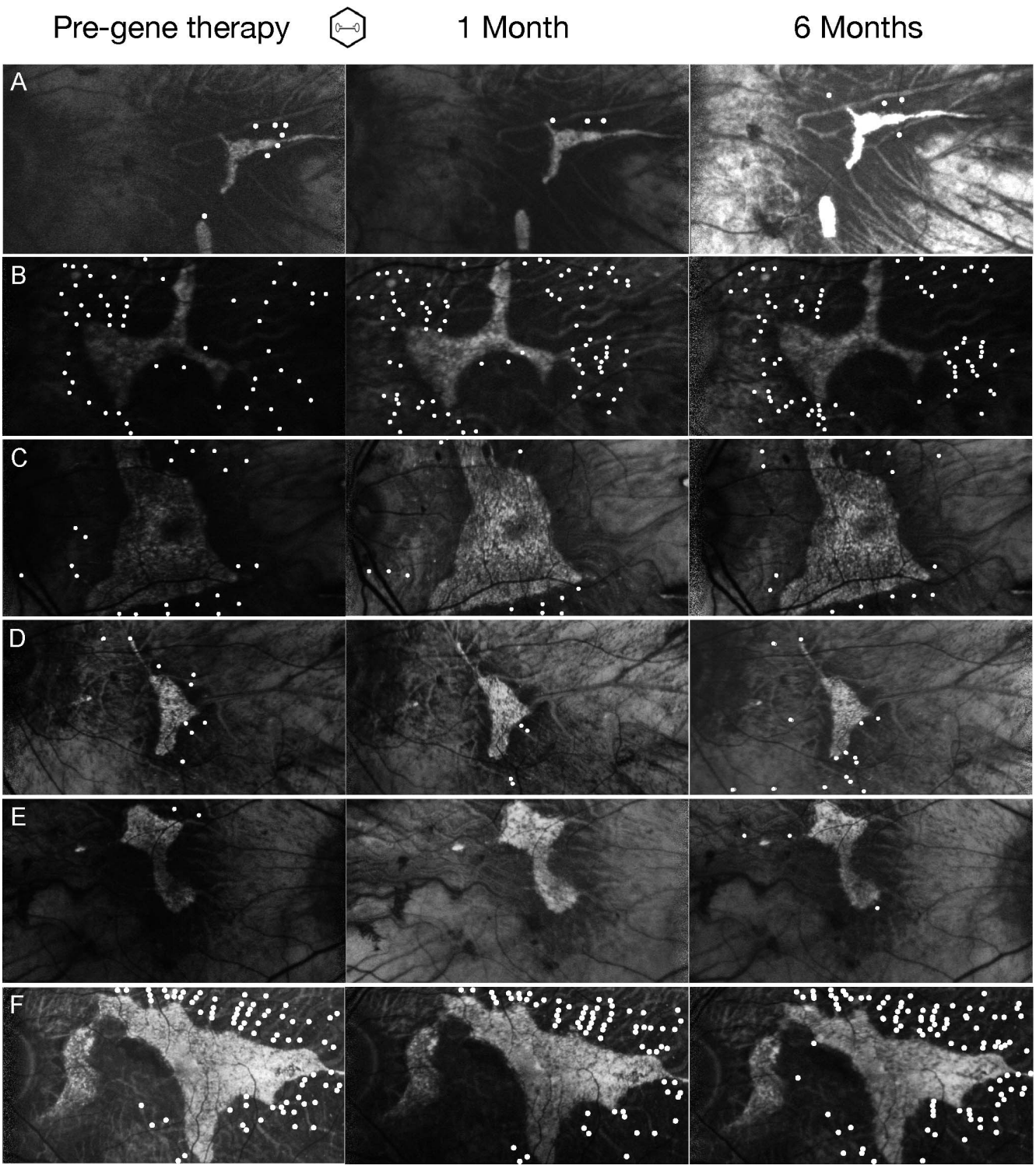

Figure 5. The effects of subretinal gene therapy on outer retinal tubulations. Gene therapy using recombinant AAV2-REP1 vector for choroideremia were performed on six eyes (**A**–**F**) in which the residual AF islands were surgically detached by subretinal injections. The locations of outer retinal cysts (*white dots*) seen on all B-scans of the OCTs, which represent cross-sections of tubulations, have been mapped onto the corresponding AF images at baseline (*left column*), 1 month post (*center column*) and 6 months post (*right column*) gene therapy.

from the main surviving outer retinal island. We found tubulations in the majority of choroideremia eyes, except those with near total outer retinal loss. While they appear cystic on OCT B-scans, mapping their locations to high magnification SLO images showed that they most likely represent cross-sections through long tubular structures jutting out from the edges of outer retinal degeneration. Tubulations have been described in a range of degenerative retinal disorders, including AMD, Stargardt disease, central serous retinopathy, serpiginous choroiditis, maternally inherited diabetes and deafness, gyrate atrophy, and choroideremia.[6,13,16–21] They likely represent rearrangement of photore-

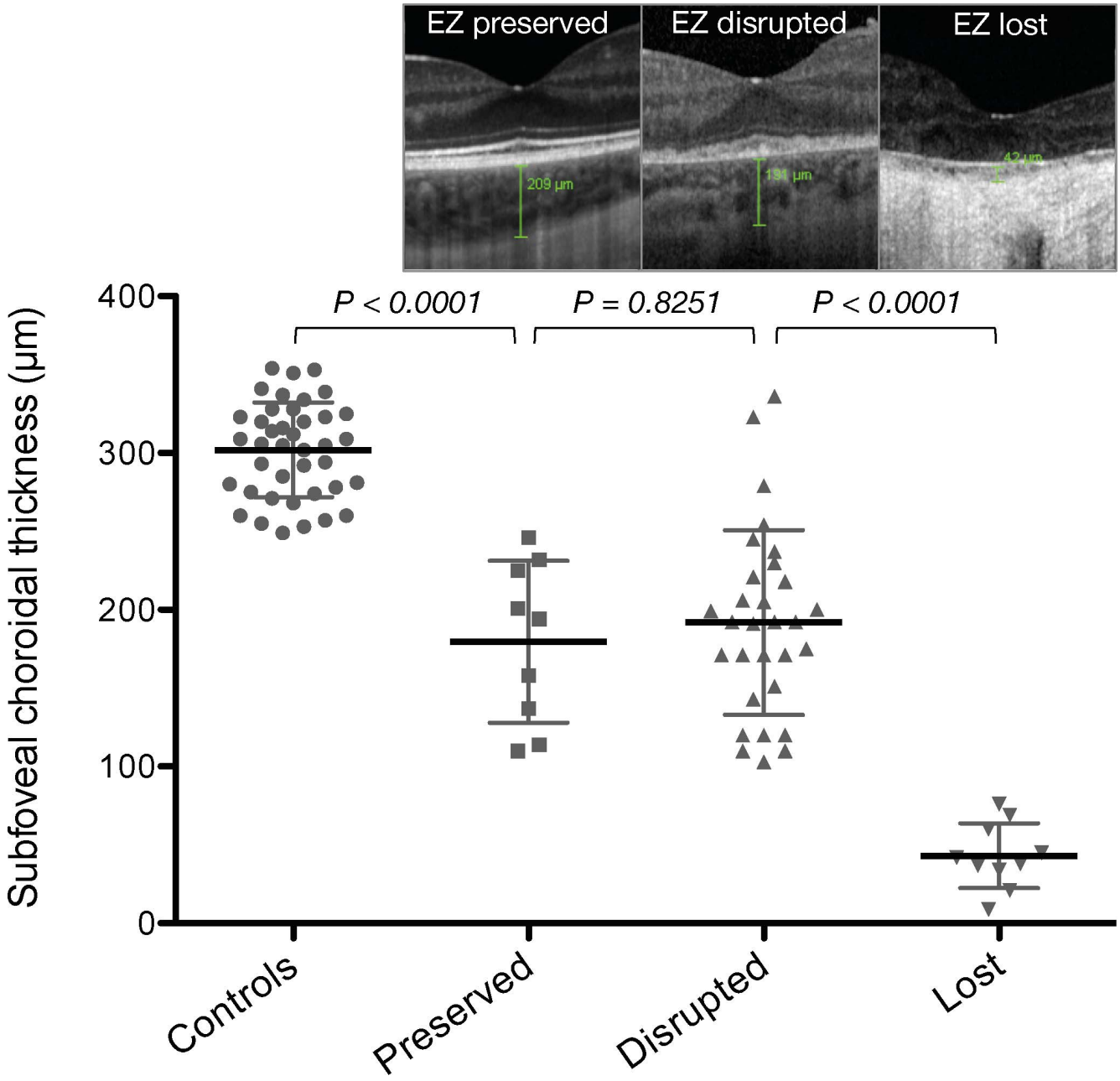

Figure 6. Scatter plot of SFCT as measured on enhanced-depth OCT in choroideremia patients with preserved, disrupted or lost ellipsoid zone (as illustrated by representative OCT images above) versus age and refractive error-matched healthy controls. The mean of each group (in *black*) is shown with 1 SD on either side (in *gray*). Intergroup statistical comparisons were performed using Kruskal-Wallis test with *P* values shown. See raw data in Supplementary Table S1.

ceptors that have lost their outer segments following the degeneration of the underlying RPE cells, but are still close enough to the residual choroid to derive oxygenation and other diffusible substrates required for metabolic survival. This would be consistent with RPE degeneration being a key feature of all the conditions above. The fact that tubulations represent residual photoreceptors is in keeping with histologic analysis of tubulations in advanced AMD, which showed cones lacking outer segments.[22] Apart from a slight dip in the total number of outer retinal cysts at 1 month post gene therapy (likely due to physical disturbance from the surgical retinal detachment), the overall numbers and distributions of tubulations were stable over a 6-month period. While this does not completely exclude the possibility of some tubulations disappearing and forming at similar locations, the data provide indirect evidence that tubulations represent stable outer retinal structures, which retain some physical attachment to the retina, rather than being inflammatory in origin.[23] The preservation of tubulations following gene therapy could also be an indication that the surgery did not cause significant disruption of outer retinal integrity, a concern due to possible stretching of the retina during subretinal injection. Because tubulations lie over bare Bruch's membrane and are often contiguous with the main retinal island, one might expect

Investigative Ophthalmology & Visual Science

Table. Choroideremia Patient Data

		OD				OS				OD	OS	
ID	**Age**	***x***	***y'***	***y***	**Δ*y***	***x***	***y'***	***y***	**Δ*y***	**Tubulation**		***CHM* Mutation (Translation)**
1	15	3699	3773	3773	0	2090	2133	2133	0	Yes	Yes	c.715C > T (pArg239X)
2	16	Outer retina off image				Outer retina off image				Yes	Yes	c.1780delC (premat term)
3	22	6386	6542	6486	56	6037	5997	5977	20	Yes	Yes	c.179delA (premat term)
4	23	3408	3447	3447	0	1714	1714	1714	0	Yes	Yes	c.715C > T (pArg239X)
5	23	5294	5406	5406	0	Outer retina off image				Yes	Yes	c.819+1G > A (intron 6 donor splice site)
6	23	5420	5996	5943	53	5519	5900	5900	0	Yes	Yes	–
7	25	Outer retina off image				Outer retina off image				Yes	Yes	c.808C > T
8	26	3210	3208	3244	−36	3269	3292	3292	0	Yes	Yes	c.1099_1100insTACC
9	27	4713	5028	4976	52	3256	3225	3225	0	Yes	Yes	c.808C > T
10	32	1924	1674	1672	2	2432	2459	2459	0	Yes	Yes	del exon/intron 9
11	32	673	741	778	−37	No outer retina remaining				Yes	Yes	c.(1245-?)del exon 10-15
12	33	3480	3826	3776	50	Poor image quality				Yes	Yes	del exon 1 exon 15
13	34	1398	1454	1454	0	302	322	322	0	Yes	Yes	del exon/intron 9
14	34	1452	1477	1477	0	1693	1707	1747	−40	Yes	Yes	c.877C > T
15	36	2852	3099	3099	0	2808	3062	3062	0	Yes	Yes	–
16	38	2207	2245	2245	0	2132	2135	2100	35	Yes	Yes	c.492_493delGA (premat term)
17	39	2770	2717	2684	33	Poor image quality				Yes	Yes	c.799C > T (p.Arg267X)
18	42	No outer retina remaining				Poor image quality				Yes	No	c.877C > T
19	42	No outer retina remaining				1021	1062	1062	0	Yes	Yes	–
20	45	No outer retina remaining				898	917	917	0	No	Yes	c.655C > T (premat term)
21	45	688	666	666	0	1923	1966	1955	11	Yes	Yes	c.130G > T (premat term)
22	46	No outer retina remaining				No outer retina remaining				No	No	c.715 C > T (pArg239X)
23	46	2836	3217	3217	0	3562	3832	3884	−52	Yes	Yes	c.1762_1765del (premat term)
24	47	990	1122	1187	−65	No outer retina remaining				Yes	Yes	c.877C > T (p.Arg293X)
25	50	No outer retina remaining				Poor image quality				Yes	–	c.1300_1303delGTGG (premat term)
26	50	No outer retina remaining				3564	3700	3639	213	Yes	Yes	c.872_880del (deletion of 4 amino acids)
27	50	2087	2059	1997	62	2635	2574	2521	53	Yes	Yes	c.189+1 G > C (exon 3 splice donor site)
28	55	No outer retina remaining				Poor image quality				Yes	Yes	c.116+1G > A (splice donor site)
29	57	No outer retina remaining				Poor image quality				Yes	Yes	c.535_538delGAAA
30	58	1454	1467	1467	0	3522	3555	3555	0	Yes	Yes	c.173G > A (p.Trp58X)
31	59	2210	2273	2249	24	2901	2986	2953	33	Yes	Yes	c.819+1G > T (intron 6 splice site)
32	59	Outer retina off image				3777	3937	3937	0	Yes	Yes	c.715C > T (pArg239X)
33	59	3049	3267	3267	0	963	1004	1004	0	Yes	Yes	c.715C > T
34	59	762	757	757	0	No outer retina remaining				Yes	Yes	c.877C > T (premat term)
35	61	225	231	231	0	1120	1132	1132	0	Yes	Yes	–
36	63	317	315	339	−24	Poor image quality				Yes	Yes	–
37	66	No outer retina remaining				No outer retina remaining				Yes	No	c.940+2T > C (intron 7 splice site)
38	71	949	969	969	0	No outer retina remaining				Yes	No	c.757C > T (Arg253X)
39	74	1921	1908	1908	0	Poor image quality				Yes	Yes	–

Optical coherence tomography and AF images of 78 eyes from 39 choroideremia patients were analyzed, of which 49 were suitable for alignment analysis. The reasons for exclusion of certain images are stated below. Transfoveal intact ONL width (*x*) was used to predict the transfoveal AF island width (see schematic drawing in Fig. 1D). The difference between the predicted (*y'*) and measured (*y*) AF island width (Δ*y*) was calculated (all measurements in μm). Mean Δ*y* was 5.94 μm (± 3.92 SEM).

retinal detachment to be induced with greater ease at these locations compared with more adherent degenerative retina elsewhere. What remains to be seen, however, is whether or not visual function can be restored in these tubulations following gene therapy and more importantly, whether or not this represents a degree of degeneration in choroideremia that may be arrested.

Acknowledgments

The data has been presented as a poster at the Oxford Ophthalmological Congress, Oxford, United Kingdom (5–8 July 2015).

Supported by National Institute of Health Research (NIHR; Whitehall, London, UK), Royal College of Surgeons of Edinburgh (London, UK), The Wellcome Trust and UK Department of Health (Grant no. HICF-091984; London, UK), NIHR Oxford Biomedical Research Centre (MO; Oxford, UK), Oxford Nuffield Medical Fellowship (TLE; Nuffield Trust, London, UK).

Disclosure: **K. Xue**, None; **M. Oldani**, None; **J.K. Jolly**, None; **T.L. Edwards**, None; **M. Groppe**, None; **S.M. Downes**, None; **R.E. MacLaren**, NightstaRx Ltd. (E)

References

1. Jolly JK, Edwards TL, Moules J, Groppe M, Downes SM, MacLaren RE. A qualitative and quantitative assessment of fundus autofluorescence patterns in patients with choroideremia. *Invest Ophthalmol Vis Sci*. In press.
2. MacLaren RE, Groppe M, Barnard AR, et al. Retinal gene therapy in patients with choroideremia: initial findings from a phase 1/2 clinical trial. *Lancet*. 2014;83:1129–1137.

3. Spaide RF, Curcio CA. Anatomical correlates to the bands seen in the outer retina by optical coherence tomography: literature review and model. *Retina*. 2011;31:1609–1619.
4. Curcio CA, Sloan KR, Kalina RE, et al. Human photoreceptor topography. *J Comp Neurol*. 1990;292:497–523.
5. Morgan JI, Han G, Klinman E, et al. High-resolution adaptive optics retinal imaging of cellular structure in choroideremia. *Invest Ophthalmol Vis Sci*. 2014;55:6381–6397.
6. Zweifel SA, Engelbert M, Laud K, et al. Outer retinal tubulation: a novel optical coherence tomography finding. *Arch Ophthalmol*. 2009;127:1596–1602.
7. Tolmachova T, Anders R, Abrink M, et al. Independent degeneration of photoreceptors and retinal pigment epithelium in conditional knockout mouse models of choroideremia. *J Clin Invest*. 2006;116:386–394.
8. Tolmachova T, Wavre-Shapton ST, Barnard AR, et al. Retinal pigment epithelium defects accelerate photoreceptor degeneration in cell type-specific knockout mouse models of choroideremia. *Invest Ophthalmol Vis Sci*. 2010;51:4913–4920.
9. Roorda A, Zhang Y, Duncan JL. High-resolution in vivo imaging of the RPE mosaic in eyes with retinal disease. *Invest Ophthalmol Vis Sci*. 2007;48:2297–2303.
10. Barteselli G, Bartsch DU, Viola F, et al. Accuracy of the Heidelberg Spectralis in the alignment between near-infrared image and tomographic scan in a model eye: a multicenter study. *Am J Ophthalmol*. 2013;156:588–592.
11. Jacobson SG, Cideciyan AV, Sumaroka A, et al. Remodelling of the human retina in choroideremia: rab escort protein 1 (REP-1) mutations. *Invest Ophthalmol Vis Sci*. 2006;47:4113–4120.
12. Lazow MA, Hood DC, Ramachandran R, et al. Transition zones between healthy and diseased retina in choroideremia (CHM) and Stargardt disease (STGD) as compared to retinitis pigmentosa (RP). *Invest Ophthalmol Vis Sci*. 2011;52:9581–9590.
13. Syed N, Smith JE, John SK, et al. Evaluation of retinal photoreceptors and pigment epithelium in a female carrier of choroideremia. *Ophthalmology*. 2001;108:711–720.
14. Laviers H, Zambarakji H. Enhanced depth imaging-OCT of the choroid: a review of the current literature. *Graefes Arch Clin Exp Ophthalmol*. 2014;252:1871–1883.
15. Sigler EJ, Randolph JC. Comparison of macular choroidal thickness among patients older than age 65 with early atrophic age-related macular degeneration and normals. *Invest Ophthalmol Vis Sci*. 2013;54:6307–6313.
16. Wolff B, Matet A, Vasseur V, et al. En face OCT imaging for the diagnosis of outer retinal tubulations in age-related macular degeneration. *J Ophthalmol*. 2012;2012:542417.
17. Sergouniotis PI, Davidson AE, Lenassi E, et al. Retinal structure, function, and molecular pathologic features in gyrate atrophy. *Ophthalmology*. 2012;119:596–605.
18. Gallego-Pinazo R, Marsiglia M, Mrejen S, et al. Outer retinal tubulations in chronic central serous chorioretinopathy. *Graefes Arch Clin Exp Ophthalmol*. 2013;251:1655–1656.
19. Raja MS, Goldsmith C, Burton BJ. Outer retinal tubulations in maternally inherited diabetes and deafness (MIDD)-associated macular dystrophy. *Graefes Arch Clin Exp Ophthalmol*. 2013;251:2265–2267.
20. Goldberg NR, Greenberg JP, Laud K, et al. Outer retinal tubulation in degenerative retinal disorders. *Retina*. 2013;33:1871–1876.
21. Mateo-Montoya A, Wolff B, Sahel JA, et al. Outer retinal tubulations in serpinginous choroiditis. *Graefes Arch Clin Exp Ophthalmol*. 2013;251:2657–2658.
22. Schaal KB, Freund KB, Litts KM, et al. Outer retinal tubulation in advanced age-related macular degeneration: optical coherence tomographic findings correspond to histology. *Retina*. 2015;35:1339–1350.
23. Wolff B, Maftouhi MQE, Mateo-Montoya A, et al. Outer retinal cysts in age-related macular degeneration. *Acta Ophthalmologica*. 2011;89:496–499.

Investigative Ophthalmology & Visual Science